Journal Pre-proof

Sulfonated graphene oxide from petrochemical waste oil for efficient conversion of fructose into levulinic acid

Chosel P. Lawagon, Kajornsak Faungnawakij, Sira Srinives, Sutarat Thongratkaew, Kawisa Chaipojjana, Araya Smuthkochorn, Patcharaporn Srisrattha, Tawatchai Charinpanitkul

PII: S0920-5861(20)30095-X

DOI: https://doi.org/10.1016/j.cattod.2020.02.036

Reference: CATTOD 12704

To appear in: *Catalysis Today*

Received Date: 30 September 2019

Revised Date: 12 January 2020

Accepted Date: 24 February 2020

Please cite this article as: Lawagon CP, Faungnawakij K, Srinives S, Thongratkaew S, Chaipojjana K, Smuthkochorn A, Srisrattha P, Charinpanitkul T, Sulfonated graphene oxide from petrochemical waste oil for efficient conversion of fructose into levulinic acid, *Catalysis Today* (2020), doi: https://doi.org/10.1016/j.cattod.2020.02.036

APCAT-8 : Abstract No. P-EF-103

Sulfonated graphene oxide from petrochemical waste oil for efficient conversion of fructose into levulinic acid

*Chosel P. Lawagon[1], Kajornsak Faungnawakij[2], Sira Srinives[3], Sutarat Thongratkaew[2], Kawisa Chaipojjana[2], Araya Smuthkochorn[1], Patcharaporn Srisrattha[1], and Tawatchai Charinpanitkul[1,4]**

[1] Center of Excellence in Particle Technology, Department of Chemical Engineering, Faculty of Engineering, Chulalongkorn University, Bangkok 10330, Thailand

[2] National Nanotechnology Center (NANOTEC), National Science and Technology Development Agency (NSTDA), 111 Thailand Science Park, Pathum Thani 12120, Thailand

[3] Chemical Engineering Department, Mahidol University, 25/25 Puttamonthon 4 Road, Nakorn Pathom 73170, Thailand

[4] Research Network of NANOTEC-KU on Nanocatalyst and Nanomaterials for Sustainable Energy and Environment, Bangkok, 10900, Thailand

*Corresponding authors: * ctawat@chula.ac.th*

Tel.: (66)-2-218-6480; Fax: (66)- 2-218-6481

Graphical Abstract

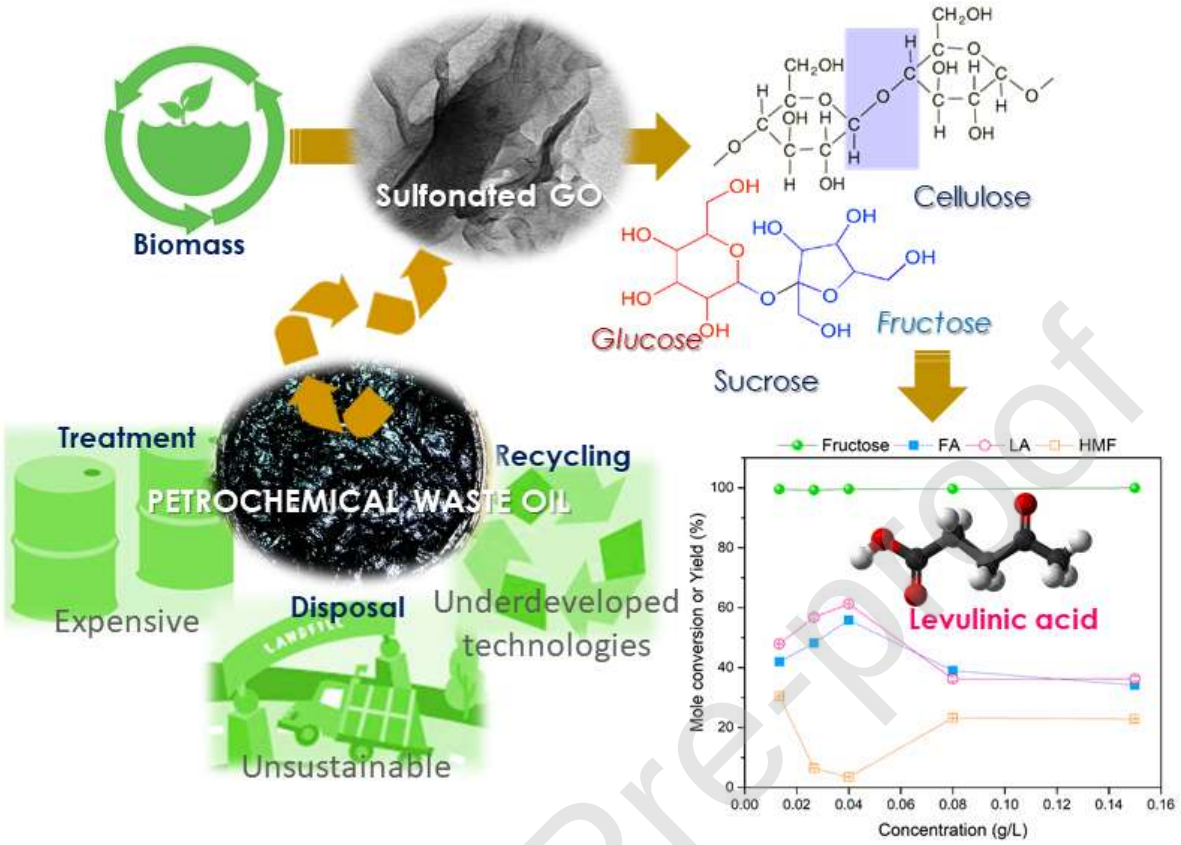

Transformation of petrochemical waste oil to sulfonated graphene oxide for efficient conversion of fructose into levulinic acid

Highlights

- Sulfonated graphene oxide was successfully synthesized from petrochemical waste oil.
- sGO has high surface area (246 m^2 g^{-1}) due to mesoporosity and many sulfonic groups.
- Recyclable sGO was successfully used for fructose conversion to levulinic acid.
- Highest yield of levulinic acid (61 %) was obtained at 160 ^oC, 1 h, and F:C=6 g g^{-1}.
- The sGO derived from petrochemical waste oil is an environmentally benign catalyst.

Abstract

Handling of petrochemical waste oil (PWO) is costly, tedious, and risky to human health and environment. Hence, upcycling of PWO for biomass conversion to platform chemicals would be very advantageous. Herein, a highly porous sheet-like structure of sulfonated graphene oxide (sGO) catalyst was synthesized from PWO. The synthesized sGO possessed high surface area (246.2 m^2 g^1) due to its mesoporosity and high content of sulfonic groups (2.4 mmol g^{-1}) grafted onto its surface. As its application, the synthesized sGO was employed to convert fructose to levulinic acid (LA) within deionized water. The high yield (61.2 mol %) of LA was obtained under a condition of 160 °C, 1 h, and 6 g g^{-1} fructose to sGO weight ratio. It can be reused several times (5 runs) with no severe degradation of catalytic activity. Therefore, the sGO derived from petrochemical waste oil would be considered as an environmentally benign catalyst for producing platform chemicals, i.e. LA from fructose and other biomass derivatives.

Keywords: sulfonated graphene oxide, catalyst, petrochemical waste oil, fructose, levulinic acid

1 Introduction

Heavy reliance on depleting fossil resources to produce platform chemicals and fuels contributes to the economic dilemma and rising emission of greenhouse gases [1-3]. Hence, alternative ways including utilization of biomass in integrated biorefineries have been explored to compete with fossil-based refineries [4]. Biomass is a renewable resource that can be exploited to produce many high value-added products, i.e. alcohol, 5-hydroxymethylfurfural (5-HMF), furfural, formic acid (FA) and levulinic acid (LA) [5, 6]. LA is considered as top ten platform chemicals, which could be further utilized to produce succinic acid, resins, polymers, herbicides, pharmaceuticals, flavoring agents, solvents, plasticizers, anti-freeze agents and biofuels/oxygenated fuel additives [3, 7]. Generally, conversion of biomass into LA involves multiple steps, which are (1) hydrolysis of cellulose to glucose, (2) isomerization of glucose to fructose, (3) dehydration of fructose to HMF, and (4) further hydrolysis to form equimolar LA and FA [2, 8]. These processes are often realized through chemical or enzymatic routes. Nevertheless, the chemical route has been recognized as high potential for commercially viable LA production [9, 10].

In the past, homogeneous acid catalysts (e.g. H_2SO_4, HCl, H_3PO_4) were used to ensure a high conversion of reactants because of lower mass transfer resistance [11]. However, those acidic catalysts are corrosive, detrimental to the environment, and non-recyclable [8, 10, 12]. Hence, heterogeneous solid acid catalysts, such as ion-exchange resins, sulfated metal oxides, modified mesoporous silica, zeolites, and natural clays have been developed to overcome the disadvantages of those homogeneous acid catalysts [13, 14]. Recently, several of these types of catalysts have been used for conversion of fructose to LA from actual biomass [15-17]. It should be noted that the acidity of heterogeneous catalysts plays a critical role in the

hydrothermal conversion of fructose to LA [18-20]. In addition, grafting of sulfonic groups has been most widely used due to high catalytic activity and LA yield [6, 8, 21]. However, the accessibility of active sites available on the surface of such heterogeneous catalysts could probably be hindered by the mass transfer resistance, resulting in poor catalytic performance [4, 11].

Novel carbon nanomaterials including graphene oxide (GO) has been recognized as a promising catalyst when compared to conventional porous catalysts due to its high surface area and the presence of active functional groups (COOH, OH) [13, 22, 23]. Sulfonated GO (sGO) is recognized as a powerful acid catalyst for biomass conversion [6, 22]. Grafting of sulfonic acid onto the two-dimensional structure of GO could lead to a large number of accessible active sites beneficial for the conversion of biomass and derivatives to high value-added platform chemicals, i.e. LA and its derivatives. Instead of using conventional disposal, which can be a cause of environmental and health threats, petroleum waste oil (PWO) was utilized to produce GO prior to its subsequent functionalization to produce sGO [24]. The as-prepared sGO was then utilized for converting fructose to LA within a high-pressure stainless-steel reactor. A systematic study was conducted to explore the effect of time, temperature, catalyst loading, and initial concentration of fructose on the catalytic performance of the synthesized sGO.

2 Experimental

2.1 Materials

Heavy fuel oil (HFO) supplied from PTT Oil and Retail Business Public Company Ltd (Batch No. TA 01/19/0004) was utilized as a representative of PWO. Sulfuric acid (98% H_2SO_4, QReC New Zealand) was used for partial carbonization of HFO. Manganese nitrate (≥99% $Mn(NO_3)_2$, Sigma-Aldrich, USA) and ethanol (99%, Aldrich USA) were used for the

graphitization of carbonized solid product (CSP). Hydrochloric acid (37% HCl, QReC New Zealand), potassium permanganate (99.0% $KMnO_4$, Ajax Finechem, Australia), sodium nitrate (99.0% $NaNO_3$, Elago Enterprises Pty Ltd, Australia), hydrogen peroxide (30% H_2O_2, QReC New Zealand), chloroform (99.8%, RCI Labscan, Thailand), and chlorosulfonic acid (≥ 99%, Merck Germany) were used for converting CSP to sGO. Catalytic performance of the synthesized sGO was examined by using D (-) Fructose (≥99%, Sigma-Aldrich USA) as feedstock for producing LA. All of the mentioned chemicals were used as received.

2.2 Synthesis of sulfonated graphene oxide (sGO)

Sulfuric acid was mixed with HFO (4:1 wt acid/wt oil) at 100 °C and mildly stirred for 1 h. Deionized water (DI) was added to the mixture (1:2 wt DI/wt mixture) and stirred for another 0.5 h. The liquid mixture was transferred to a Teflon-lined stainless autoclave reactor, which was heated to a designated temperature of 180 °C for 24 h. After it cooled down to room temperature, a dark black suspension was filtered, washed with DI water, and dried in an oven at 80 °C for 12 h, resulting in the carbonized solid product (CSP). The CSP was then impregnated with $Mn(NO_3)_2$ solution in ethanol (~6 mmol metal g^{-1} C) and subject to thermal treatment at 900 °C (5 °C min^{-1}, 3 h) under N_2 atmosphere [25]. The CSP powder was washed with HCl (10% v/v) to remove residual manganese radicals [26]. The graphitized solid product (GSP) was used as a precursor for the production of GO powder using a modified Hummer's method [27]. Then sulfonation of the GO powder was conducted by suspending it in chloroform, mixed with chlorosulfonic acid (2:1 wt/wt) under continuous stirring, and being refluxed at 70 °C for 4h. Finally, the resultant sulfonated GO (sGO) was then filtered, washed with ethanol and DI water until neutral pH, and dried at 105 °C for 12 h.

2.3 Catalysts characterization

The degree of functionalization of the resultant sGO sample was determined via Fourier transform infrared (FTIR) spectroscopy (FTS 6000 FTIR spectrometer, Bio-rad, USA), Raman spectroscopy (laser frequency of 514 nm, DXR Raman system, Thermo Fisher Scientific, USA), and X-ray photoelectron spectroscopy (ESCALAB 250Xi, Fisher Scientific, USA). The acidity distribution was analyzed by the Boehm titration method [28]. The elemental composition of the as-prepared sGO sample was also characterized (LECO 628, UK). Morphology of the synthesized sGO was observed under Scanning Electron Microscope (SEM-EDX, Hitachi S-3500 N, Japan) and Transmission Electron Microscope (TEM, Hitachi H-7650, Japan). Brunauer-Emmett-Teller (BET) specific surface area analysis was carried out using Belsorp-mini II (Bel Japan, Inc.). Nitrogen adsorption/desorption isotherms were measured at relative pressure range ($p\ p_o^{-1}$) between 0.01 and 1.0. Meanwhile, the pore size distribution was determined using the Barrett-Joyner-Halenda (BJH) method.

2.4 Catalytic Test

In each test, fructose and sGO catalyst were mixed in 30 mL of deionized water and loaded into a high-pressure stainless-steel reactor (50 ml) equipped with a temperature controller and a magnetic stirrer. Effect of reaction time, temperature, catalyst loading, and initial concentration of fructose on the catalytic performance of the synthesized sGO was examined at a constant stirring speed of 300 rpm. For the recyclability test, the catalyst was regenerated after each run by washing with DI water and acetone to remove residual organic compounds and then dried in an oven overnight at 80 °C. The reactor was instantaneously quenched to terminate all reactions. Liquid sample was then drawn from the reactor and syringe filtered (13 mm, 0.45 μm, Whatman). The chemical composition of the filtered liquid sample was analyzed using HPLC with an Aminex sugar column (HPX-87H sugar 300 × 7.8 mm, Bio-Rad, Hercules, CA). 5 mM H_2SO_4 was used as a mobile phase at 0.6 ml min^{-1}. The fructose

conversion and LA yield could be determined based on the initial amount (F_i) and final amount (F_f) of fructose remaining after reaction as described in Eqs. 1 and 2, respectively.

$$Fructose\ conversion\ (mol\ \%) = \frac{F_i - F_f}{F_i}\ x\ 100\% \quad (1)$$

$$LA\ yield\ (mol\ \%) = \frac{moles\ of\ produced\ LA}{F_i}\ x\ 100\% \quad (2)$$

3. Results and Discussion

3.1 Characterization of sGO catalyst

Fig. 1(a) and **(b)** exhibit the microscopic appearance of CSP and GSP, respectively. CSP is a conglomeration of porous carbonaceous solid with mainly graphitic and amorphous carbon content. After graphitization, the resultant GSP exhibited a particulate form with high graphitic carbon content and higher porosity. Then graphene oxide (GO) which was prepared from GSP by the modified Hammer's method displayed a fine powdery appearance. Similarly, the resultant sGO, which was prepared from the GO functionalized with the sulfonic group, also exhibited the particulate form. The TEM image of GO depicted in **Fig. 1(c)** suggests sheet-like morphological property while the sGO became more wrinkled probably due to sulfonation as shown in **Fig. 1(d)**. The transparency observed in the TEM images suggests the formation of few-layer stacking of graphene sheets correlating to its high surface area. These results could confirm that the sulfonation step exerted insignificant change in the microscopic structure of sGO when compared to that of GO [11].

<<< **Please insert Fig. 1** >>>

Nevertheless, successful functionalization could be confirmed by FTIR analysis as shown in **Fig. 2(a)**. For comparison, the typical sample of GO shows characteristic peaks of C=O stretching (1727 cm^{-1}), O-H deformation (1402 cm^{-1}), C-OH stretching (1225 cm^{-1}) and C-O stretching vibration (1050 cm^{-1}) [29]. Unoxidized graphitic domains (1,620 cm^{-1}) could be

detected in both GO and sGO samples with attenuated bands (1,620, 1,225, and 1,050 cm^{-1}) in sGO spectrum due to reduction during sulfonation [29, 30]. The presence of sulfonic acid group (−SO_3H) on the surface of the synthesized sGO can be confirmed with the appearance of a distinct band at the wavenumber of 1,030 cm^{-1} [29, 31]. Furthermore, with the Boehm titration method, it could be confirmed that both GO and sGO samples contained abundant acid sites (**Table 1**). Sulfonic groups could be quantified based on the S content in the sample determined through elemental analysis. As summarized in **Table 2**, significantly higher sulfur content in the sGO sample (7.58 %) compared to that in the GO sample (1.54 %) confirmed the effective sulfonation. It should be noted that an initial sulfur content in the GO sample would be attributed to usage of H_2SO_4 for the exfoliation of the GSP sample via Hummer's method [31]. The incorporation of elemental sulfur in the GO sample was further verified with the occurrence of the S 2p signal at 168.3 eV associated with a S=O band in the XPS spectra (**Fig. 2(b)**) [4, 32]. The signals of C 1s and O 1s in the spectra confirms the presence of oxygen-containing groups (C–C, C–O, C=O and COOH) [4, 11]. The observed increased in intensity of the absorption peaks for C1s (~285 eV) in sGO sample is due to removal of oxygen functional groups after sulfonation [6]. Thereby, eliminating the possibility that the C 1s peak is solely due to oil vapor contamination. Uniform dispersion of the sulfonic functional group in the GO surface was also verified through EDX analysis (**Fig. S1**). On the other hand, the graphitic nature of both GO and sGO samples were characterized by D-band and G-band observed in the Raman spectra (**Fig. 2(c)**) indicating sp^2 carbon in 2D hexagonal lattice and sp^3carbon atoms of defects and disorder respectively [33, 34]. The distinctly higher intensity of the D-band in the GO sample suggested the presence of disorder carbonaceous content which was grafted with oxygen functional groups during Hummer's process [35]. However, a decrease in intensity ratio of D-band to G-band (I_D/I_G) from 1.06 (GO) to 0.67 (sGO) indicates the higher content of graphitic carbon in the sGO sample

resulted from the reduction during the sulfonation process [34, 36]. As shown in **Fig. 2(d)**, specific surface area of the sGO sample was elevated significantly to 246.18 m^2 g^{-1} when compared to that of the GO sample (181.13 m^2 g^{-1}). This result would be ascribed to the presence of higher portion of mesopores in the sGO sample (**Fig. 1(d) inset**) which could also be confirmed by the N_2 adsorption-desorption isotherms (Type-IV isotherm with H3-type hysteresis) [37, 38].

<<< **Please insert Fig. 2** >>>

<<< **Please insert Table 1** >>>

<<< **Please insert Table 2** >>>

3.2 Conversion of fructose to levulinic acid

Conversion of fructose to levulinic acid (LA, **Fig. S2**) could be initiated with the opening of the cyclic hexose structure and then it undergoes enolization and dehydration to yield 5-HMF [39, 40]. This first stable dehydration product is hydrolyzed to yield equimolar linear molecules, LA and FA [39]. A detectable amount of humins as a byproduct is also produced in a typical homogeneous catalyst, such as sulfuric acid [16]. The separation of LA, byproducts, and sulfuric acid, would require tedious steps and high energy consumption. Therefore, heterogeneous catalysts including sGO are of interest to many research teams [4, 6, 8, 9, 11, 12, 14]. However, confirmable understanding in the effect of reaction time, temperature, catalyst loading, and initial fructose concentration is essential for determining the efficiency of such heterogeneous catalyst in converting fructose to LA.

3.2.1. Effect of reaction time

As shown in **Fig. 3** significant fast conversion of fructose to LA could be observed when the sGO catalyst was employed at 200 °C with DI as a solvent. In the first 10 mins, fructose

conversion was already at 97.0% with the presence of 1.2% unconverted 5-HMF and 26.9% LA yield. When the reaction further proceeded within the first 60 mins yield of LA as well as FA was gradually increased, and fructose conversion reached ~100%. However, yield of 5-HMF was significantly decreased as the reaction time was prolonged attesting the formation of intermediate products and eventually LA and FA. Meanwhile, yields of LA and FA were also decreased when the system was further operated for 120 mins, suggesting that 5-HMF would take part in humin formation through the aldehyde and hydroxyl reactive sites [18, 42, 43]. Therefore, with the presence of sGO catalyst almost full conversion of fructose could be achieved within 60 mins, resulting in the LA yield of 38.5% but the excessively long reaction time would inevitably promote byproduct formation. The same case was also observed when an actual biomass was used for the one-pot conversion to LA [15].

<<< **Please insert Fig. 3** >>>

3.2.2 Effect of temperature

From a kinetic point of view, the temperature dependence of the formation of LA and other relevant products is a key issue for evaluating the performance of the prepared catalyst. It is evident that while fructose conversion was rather stable, the formation of LA relied on the reaction temperature (**Fig. 4**). At the lowest reaction temperature of 140 °C, a nominal yield of LA was about 29.7%. Meanwhile, a maximum LA yield of 41.0% was attained at 160 °C. However, a further increase in the reaction temperature to 180 and 200 °C would result in a decrease in the LA yield. The highest yield of 5-HMF (10.42%) was obtained at the reaction temperature of 140 °C but only a trace amount of 5-HMF was detected at the reaction temperature ≥ 160 °C. These results would suggest that the rate of fructose conversion was stable while the conversion of 5-HMF to LA and FA would be significantly enhanced with

the elevation of the reaction temperature [44]. The stable fructose conversion at any reaction temperature would signify that the increase in the reaction temperature would affect only the secondary reactions which result in other side products. It was also reported that 5-HMF could simultaneously participate in the production of humins and other side products with an increase in the reaction temperature [41-44]. Based on the thermodynamic viewpoint ($E_a = \Delta H + RT$), the reaction activation energy (E_a) would depend on the reaction temperature (T) and enthalpy change. The conversion of 5-HMF to LA would require higher enthalpy change (ΔH) when compared to the conversion fructose to 5-HMF [41]. Therefore, the conversion of fructose to 5-HMF would be less sensitive to the reaction temperature because ΔH could overshadow the temperature dependency of fructose conversion. On the other hand, subsequent conversion of 5-HMF to LA and FA would be more temperature-sensitive, as the enthalpy changes, resulting in a significant decrease in 5-HMF yield. This result would be supported by similar findings where conversion of fructose with dilute acid catalyst achieved an optimal value when the reaction temperature was above 180 °C [9, 45]. When compared with those previous results, the usage of the sGO catalyst synthesized from petrochemical waste oil would be more effective for fructose conversion to LA because the highest yield of LA could be achieved at lower reaction temperature.

<<< **Please insert Fig. 4** >>>

3.2.3 Effect of catalyst loading

According to the heterogeneity, the amount of catalyst loaded into the reactor would exert significant effect on reactant conversion due to the availability of active sites and accessibility of the reactant molecules. It should be noted that the sGO with sheet-like structure (**Fig. 1(d)**) exhibited mesoporosity with a very high surface area of 246.2 $m^2\ g^{-1}$

(**Fig. 2(d)**), resulting in excellent interaction of fructose and active sites. A high amount of oxygen-containing functionalities (**Table 1**) could enhance the hydrophilicity of the sGO surface, which would be beneficial to catalytic conversion of fructose [46]. In addition, the presence of sulfonic group (2.4 mmol g^{-1}) on the sGO surface (**Fig. 2(a)**) would also crucially enhance fructose conversion to LA. As depicted in **Fig. 5**, almost 100% of fructose conversion with the 5-HMF yield of 28.4 % and the LA yield of 17.7 % could be achieved with the sGO loading of 0.1 g. Then usage of 0.2 g of the sGO catalyst could elevate the LA yield up to 41.2 % with the lowest yield of 5-HMF. However, a further increase in the sGO loading could exert only a slight effect on the yield of 5-HMF, LA and FA. It was also reported that hydrolysis of 5-HMF to LA could be enhanced with the higher content of acid concentration [18]. Nevertheless, excessive loading of the sGO would promote not only the dehydration of fructose to LA but also the degradation of the 5-HMF and LA into other byproducts, such as humins [17, 47]. As a result, there was an optimal ratio of fructose to the sGO of 22.5 g g^{-1}, which could provide the highest LA production.

<<< **Please insert Fig. 5** >>>

3.2.4 Effect of initial fructose concentration

The excellent performance of the sGO catalyst in converting fructose could be confirmed by ~100% conversion with regard to all tested initial fructose concentration in this study as shown in **Fig. 6**. Such complete conversion regarding all of the initial fructose concentrations reveals that even the 0.2 g sGO loading could provide active sites sufficient for fructose molecules [40, 46]. Interestingly, the LA yield was gradually elevated from 47.9 to 61.2 % while the remaining yield of 5-HMF was decreased from 30.5 to 3.4 % when the initial concentration of fructose was increased from 10 to 40 g L^{-1}. Nevertheless, a further increase

in the initial concentration of fructose > 80 g L^{-1} resulted in higher yield of 5-HMF and subsequently to lower yield of LA and FA. This can be attributed to higher initial amount of carbon precursor with its full conversion only leads to large amount of humin formation noting its higher reaction order compared to LA [18]. As a result, there would be an appropriate fructose to sGO ratio at which active sites of the sGO would still be available for converting 5-HMF to LA and FA [47]. With the designated reaction temperature of 160 °C, the fructose: sGO ratio exerted an insignificant effect on the fructose conversion. As depicted in **Fig. S3**, the highest LA yield of 61.2% could be achieved with the fructose: sGO ratio of 6 g g^{-1}. However, with the fructose: sGO ratio ≥ 10 the yield of unconverted 5-HMF was increased while the LA yield was significantly decreased. These results would be attributed to the competitive rate of fructose conversion to 5-HMF and other subsequent products, which was regulated by the available active sites of the sGO catalyst [41]. As summarized in **Table 3**, hydrolysis of fructose in a pure aqueous environment achieved the LA yield of ~72 % with the presence of Dowex 50 × 8-100 resin while the LA yield of ~74% and higher LA yield was obtained when H_2SO_4 was employed as a homogeneous catalyst [2, 33, 41, 48]. However, as abovementioned such corrosive acid catalyst would inevitably pose disadvantages of environmental concerns and separation problems. In summary, the sGO catalyst synthesized from petrochemical waste oil which was employed for converting fructose as a model biomass substrate could provide a promising avenue for the utilization of hazardous wastes into a more beneficial platform for producing a high value-added product, such as LA.

<<< Please insert Fig. 6 >>>

<<< Please insert Table 3 >>>

3.2.5 Recyclability of sGO catalyst

The sGO catalyst was used for five times to confirm its stability which is an important aspect of solid heterogeneous catalysts. The regenerated catalyst after each run was weighed and constant fructose to catalyst (F:C) ratio of 6 g g^{-1} was maintained throughout all repeated runs. As shown in **Fig. 7**, the catalytic activity of sGO slightly declined in the second run then a significant decrease in the fructose conversion and LA yield was observed in the 3rd to 5th runs. Such declining activity would be ascribed to the formation of humins which are not easily removed with acetone, thereby reducing the activity of the catalyst [40]. As LA and FA yield decreased, the amount of 5-HMF increased as an intermediate product. These results could be implied with the mechanistic pathway shown in **Fig. S2** [39-41]. Amount of sulfonic groups and total acidic sites in sGO significantly decrease after five repeated runs (**Table 4**).

<<< Please insert Figure 7 >>>

<<< Please insert Table 4 >>>

As shown in **Fig. 7**, a rather stable conversion of fructose and stable yield of each product was still observed though sGO's catalytic activity would decline after several repeated runs. It should be noted that the ease of separation and recyclability would be an advantage of such heterogeneous catalyst [16]. Therefore, it would be reasonably implied that the sGO catalyst synthesized from petrochemical waste oil is a good candidate for conversion of biomass which mainly consists of fructose content.

4. Conclusions

The porous sheet-like sGO catalyst with very high surface area of 246.2 m^2 g^{-1} could be synthesized from petrochemical waste oil. The high content of sulfonic group (2.4 mmol g^{-1}) could be grafted onto the surface of GO, resulting in the formation of sGO which could provide a high yield to LA converted from fructose. Effective catalytic performance of the synthesized sGO catalyst could be confirmed with ~100% conversion of fructose and the highest yield of LA (61.2%) with the reaction temperature of 160 °C and the fructose to sGO ratio of 6 g g^{-1}. At optimal conditions, sGO was reusable up to five times with minimal degradation in catalytic activity. These results suggest that utilization of hazardous petrochemical waste oil to synthesize the sGO could thereby reduce its threat to the environment and provide a promising way for producing LA from fructose which represents a typical content of waste biomass.

Credit Author Statement

All of our coauthoring team members who meet authorship criteria are listed. All authors certify that they have participated sufficiently in this work to take public responsibility for the content, including participation in the concept, design, analysis, writing, or revision of the manuscript. Furthermore, each author certifies that this material or similar material has not been and will not be submitted to or published in any other publication before its appearance in Catalysis Today.

Declaration of Interest Statement

The authors whose names are listed immediately below certify that this manuscript is an original work. It has not been published previously or under consideration for publication elsewhere. Also, the authors would like to confirm that there is no conflict of interest among us. Also, we do not have affiliations with or involvement in any organization or entity with any financial interest (such as honoraria; educational grants; participation in speakers' bureaus; membership, employment, consultancies, stock ownership, or other equity interest; and expert testimony or patent-licensing arrangements), or non-financial interest (such as personal or professional relationships, affiliations, knowledge or beliefs) in the subject matter or materials discussed in this manuscript. Once this manuscript is accepted, it will not be published elsewhere in the same form, in any language, without the written consent of the publisher.

Acknowledgement

This research was supported by Ratchadapisek Sompoch Endowment Fund of Chulalongkorn University for Postdoctoral Fellowship (CL). Also, partial supports of Ratchadapisek

Sompoch Endowment Fund (2015) for CEPT (CU-58-064-CC) and the National Nanotechnology Center (NANOTEC), NSTDA, the Ministry of Science and Technology of Thailand through the program of Research Network of NANOTEC (RNN) were gratefully acknowledged.

Electronic Supporting Information (ESI) can be downloaded online.

References:

[1] R. Ahorsu, F. Medina, M. Constantí, Energies. 11 (2018). doi:10.3390/en11123366.

[2] Á. Szabolcs, M. Molnár, G. Dibó, L.T. Mika, Green Chem. 15 (2013) 439–445. doi:10.1039/c2gc36682g.

[3] D. Rackemann, W. Doherty, Biofuels, Bioprod. Biorefining. 5 (2011) 198-214. doi:10.1002/BBB.

[4] Q. Hou, W. Li, M. Ju, L. Liu, Y. Chen, Q. Yang, RSC Adv. 6 (2016) 104016–104024. doi:10.1039/c6ra23420h.

[5] M. Mascal, E.B. Nikitin, Green Chem. 12 (2010) 370–373. doi:10.1039/b918922j.

[6] P.P. Upare, J.W. Yoon, M.Y. Kim, H.Y. Kang, D.W. Hwang, Y.K. Hwang, H.H. Kung, J.S. Chang, Green Chem. 15 (2013) 2935–2943. doi:10.1039/c3gc40353j.

[7] D.J. Braden, C.A. Henao, J. Heltzel, C.C. Maravelias, J.A. Dumesic, Green Chem. 13 (2011) 1755–1765. doi:10.1039/c1gc15047b.

[8] D.M. Alonso, J.M.R. Gallo, M.A. Mellmer, S.G. Wettstein, J.A. Dumesic, Catal. Sci. Technol. 3 (2013) 927–931. doi:10.1039/c2cy20689g.

[9] P.A. Son, S. Nishimura, K. Ebitani, React. Kinet. Mech. Catal. 106 (2012) 185–192. doi:10.1007/s11144-012-0429-1.

[10] F.D. Pileidis, M.M. Titirici, ChemSusChem. 9 (2016) 562–582. doi:10.1002/cssc.201501405.

[11] K. Li, J. Chen, Y. Yan, Y. Min, H. Li, F. Xi, J. Liu, P. Chen, Carbon N. Y. 136 (2018) 224–233. doi:10.1016/j.carbon.2018.04.087.

[12] J. Zhao, C. Zhou, C. He, Y. Dai, X. Jia, Y. Yang, Catal. Today. 264 (2016) 123–130. doi:10.1016/j.cattod.2015.07.005.

[13] H. Wang, Q. Kong, Y. Wang, T. Deng, C. Chen, X. Hou, Y. Zhu, ChemCatChem. 6 (2014) 728–732. doi:10.1002/cctc.201301067.

[14] M.M. Antunes, P.A. Russo, P. V. Wiper, J.M. Veiga, M. Pillinger, L. Mafra, D. V. Evtuguin, N. Pinna, A.A. Valente, ChemSusChem. 7 (2014) 804–812. doi:10.1002/cssc.201301149.

[15] X. Li, R. Xu, Q. Liu, M. Liang, J. Yang, S. Lu, G. Li, L. Lu, C. Si, Ind. Crops Prod. 141 (2019) 111759. https://doi.org/10.1016/j.indcrop.2019.111759.

[16] M. Signoretto, S. Taghavi, E. Ghedini, F. Menegazzo, Molecules. 24 (2019) 1–20. https://doi.org/10.3390/molecules24152760.

[17] B. Velaga, R.P. Parde, J. Soni, N.R. Peela, Microporous Mesoporous Mater. 287 (2019) 18–28. https://doi.org/10.1016/j.micromeso.2019.05.049.

[18] D. Jung, P. Körner, A. Kruse, Biomass Convers. Biorefinery. (2019). https://doi.org/10.1007/s13399-019-00507-0.

[19] H. Qu, B. Liu, G. Gao, Y. Ma, Y. Zhou, H. Zhou, L. Li, Y. Li, S. Liu, Fuel Process. Technol. 193 (2019) 1–6. https://doi.org/10.1016/j.fuproc.2019.04.035.

[20] W. Wei, H. Yang, S. Wu, Fuel. 256 (2019) 115940. https://doi.org/10.1016/j.fuel.2019.115940.

[21] C. Pizzolitto, E. Ghedini, F. Menegazzo, M. Signoretto, A. Giordana, G. Cerrato, G. Cruciani, Catal. Today. (2019) 0–1. https://doi.org/10.1016/j.cattod.2019.11.012.

[22] S. Zhu, J. Wang, W. Fan, Catal. Sci. Technol. 5 (2015) 3845–3858. doi:10.1039/c5cy00339c.

[23] P.P. Upare, D.Y. Hong, J. Kwak, M. Lee, S.K. Chitale, J.S. Chang, D.W. Hwang, Y.K. Hwang, Catal. Today. 324 (2019) 66–72. doi:10.1016/j.cattod.2018.07.002.

[24] P. Singh, A. Ojha, A. Borthakur, R. Singh, D. Lahiry, D. Tiwary, P.K. Mishra, Environ. Sci. Pollut. Res. 23 (2016) 22340–22364. doi:10.1007/s11356-016-7373-y.

[25] M. Demir, Z. Kahveci, B. Aksoy, N.K.R. Palapati, A. Subramanian, H.T. Cullinan, H.M. El-Kaderi, C.T. Harris, R.B. Gupta, Ind. Eng. Chem. Res. 54 (2015) 10731–10739. doi:10.1021/acs.iecr.5b02614.

[26] J. Zhang, H. Yang, G. Shen, P. Cheng, J. Zhang, S. Guo, Chem. Commun. 46 (2010) 1112–1114. doi:10.1039/b917705a.

[27] J.R. Lomeda, C.D. Doyle, D. V. Kosynkin, W.F. Hwang, J.M. Tour, J. Am. Chem. Soc. 130 (2008) 16201–16206. doi:10.1021/ja806499w.

[28] S. Goertzen, K. Thériault, A. Oickle, A. Tarasuk, H. Andreas, Carbon 48 (2010) 1252–1261. doi:10.1016/j.carbon.2009.11.050.

[29] S. Park, H. Kim, J. Electrochem. Soc. 163 (2016) A2293–A2298. doi:10.1149/2.0731610jes.

[30] S. Wu, K. Zhang, X. Wang, Y. Jia, B. Sun, T. Luo, F. Meng, Z. Jin, D. Lin, W. Shen, L. Kong, J. Liu, Chem. Eng. J. 262 (2015) 1292–1302. doi:10.1016/j.cej.2014.10.092.

[32] D. He, Z. Kou, Y. Xiong, K. Cheng, X. Chen, M. Pan, S. Mu, Carbon N. Y. 66 (2014) 312–319. doi:10.1016/j.carbon.2013.09.005.

[33] Y. Shen, X. Zhu, L. Zhu, B. Chen, Chem. Eng. J. 314 (2017) 336–346. doi:10.1016/j.cej.2016.11.132.

[34] S. Perumbilavil, P. Sankar, T. Priya Rose, R. Philip, Appl. Phys. Lett. 107 (2015) 10–15. doi:10.1063/1.4928124.

[35] Y. Shen, B. Chen, Environ. Sci. Technol. 49 (2015) 7364–7372. doi:10.1021/acs.est.5b01057.

[36] S. Muhammad Hafiz, R. Ritikos, T.J. Whitcher, N. Md. Razib, D.C.S. Bien, N. Chanlek, H. Nakajima, T. Saisopa, P. Songsiriritthigul, N.M. Huang, S.A. Rahman, Sensors Actuators, B Chem. 193 (2014) 692–700. doi:10.1016/j.snb.2013.12.017.

[37] K.S.W. Sing, D.H. Everett, R. a. W. Haul, L. Moscou, R.S. Pierotti, J. Rouquerol, T. Siemieniewska, Pure Appl. Chem. 57 (1985) 603–619. doi:10.1351/pac198557040603.

[38] G. Ma, Q. Yang, K. Sun, H. Peng, F. Ran, X. Zhao, Z. Lei, Bioresour. Technol. 197 (2015) 137–142. doi:10.1016/j.biortech.2015.07.100.

[39] J. Jow, G.L. Rorrer, M.C. Hawley, D.T.A. Lamport, Biomass. 14 (1987) 185–194. doi:10.1016/0144-4565(87)90046-1

[40] I. Thapa, B. Mullen, A. Saleem, C. Leibig, R.T. Baker, J.B. Giorgi, Appl. Catal. A Gen. 539 (2017) 70–79. doi:10.1016/j.apcata.2017.03.016.

[41] L. Qi, Y.F. Mui, S.W. Lo, M.Y. Lui, G.R. Akien, I.T. Horváth, ACS Catal. 4 (2014) 1470–1477. doi:10.1021/cs401160y.

[42] H. Ren, B. Girisuta, Y. Zhou, L. Liu, Carbohydr. Polym. 117 (2015) 569–576. doi:10.1016/j.carbpol.2014.09.091.

[43] X. Hu, S. Kadarwati, S. Wang, Y. Song, M.D.M. Hasan, C.Z. Li, Fuel Process. Technol. 137 (2015) 212–219. doi:10.1016/j.fuproc.2015.04.024.

[44] V. Choudhary, S.H. Mushrif, C. Ho, A. Anderko, V. Nikolakis, N.S. Marinkovic, A.I. Frenkel, S.I. Sandler, D.G. Vlachos, J. Am. Chem. Soc. 135 (2013) 3997–4006. doi:10.1021/ja3122763.

[45] J. Su, F. Shen, M. Qiu, X. Qi, T.J. Farmer, J.H. Clark, Molecules. 22 (2017). doi:10.3390/molecules22020285.

[46] J. Ji, G. Zhang, H. Chen, S. Wang, G. Zhang, F. Zhang, X. Fan, Chem. Sci. 2 (2011) 484–487. doi:10.1039/c0sc00484g.

[47] X. Qi, N. Liu, Y. Lian, RSC Adv. 5 (2015) 17526–17531. doi:10.1039/c4ra15296d.

[48] B.A. Fachri, R.M. Abdilla, H.H.V. De Bovenkamp, C.B. Rasrendra, H.J. Heeres, ACS Sustain. Chem. Eng. 3 (2015) 3024–3034. doi:10.1021/acssuschemeng.5b00023.

List of Figures

Figure 1 SEM images of **(a)** CSP and **(b)** GSP and TEM images of **(c)** GO and **(d)** sGO

Figure 2 (a) FTIR spectra, **(b)** XPS spectra, **(c)** Raman spectra, and **(d)** N_2 adsorption-desorption isotherms of GO and sGO (pore size distribution as insert)

Figure 3 Effect of reaction time on fructose conversion and product yield (200 °C, 0.2 g catalyst, 4.5 g Fructose, 30 mL DI)

Figure 4 Effect of temperature on fructose conversion and product yield (1 h, 0.2 g catalyst, 4.5 g Fructose, 30 mL DI)

Figure 5 Effect of catalyst loading on fructose conversion and product yield (160 °C, 1 h, 4.5 g Fructose, 30 mL DI)

Figure 6 Effect of initial concentration of fructose on its conversion and product yield (160 °C, 1 h, 0.2 g catalyst, 30 mL DI)

Figure 7 Effect of repeated runs using regenerated catalyst on its conversion and product yield (160 °C, 1 h, 0.2 g catalyst, 30 mL DI)

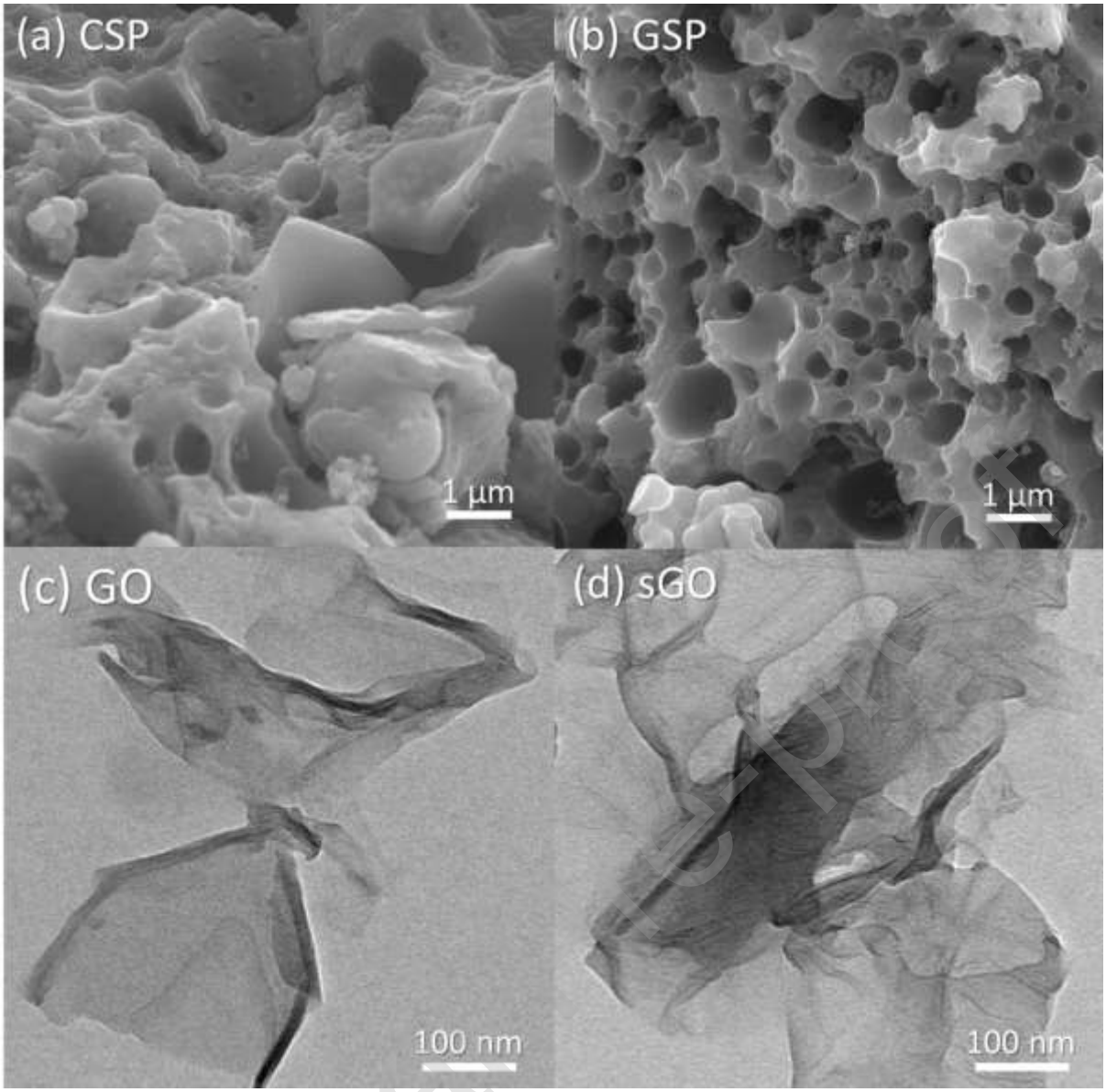

Figure 1 SEM images of **(a)** CSP and **(b)** GSP and TEM images of **(c)** GO and **(d)** sGO

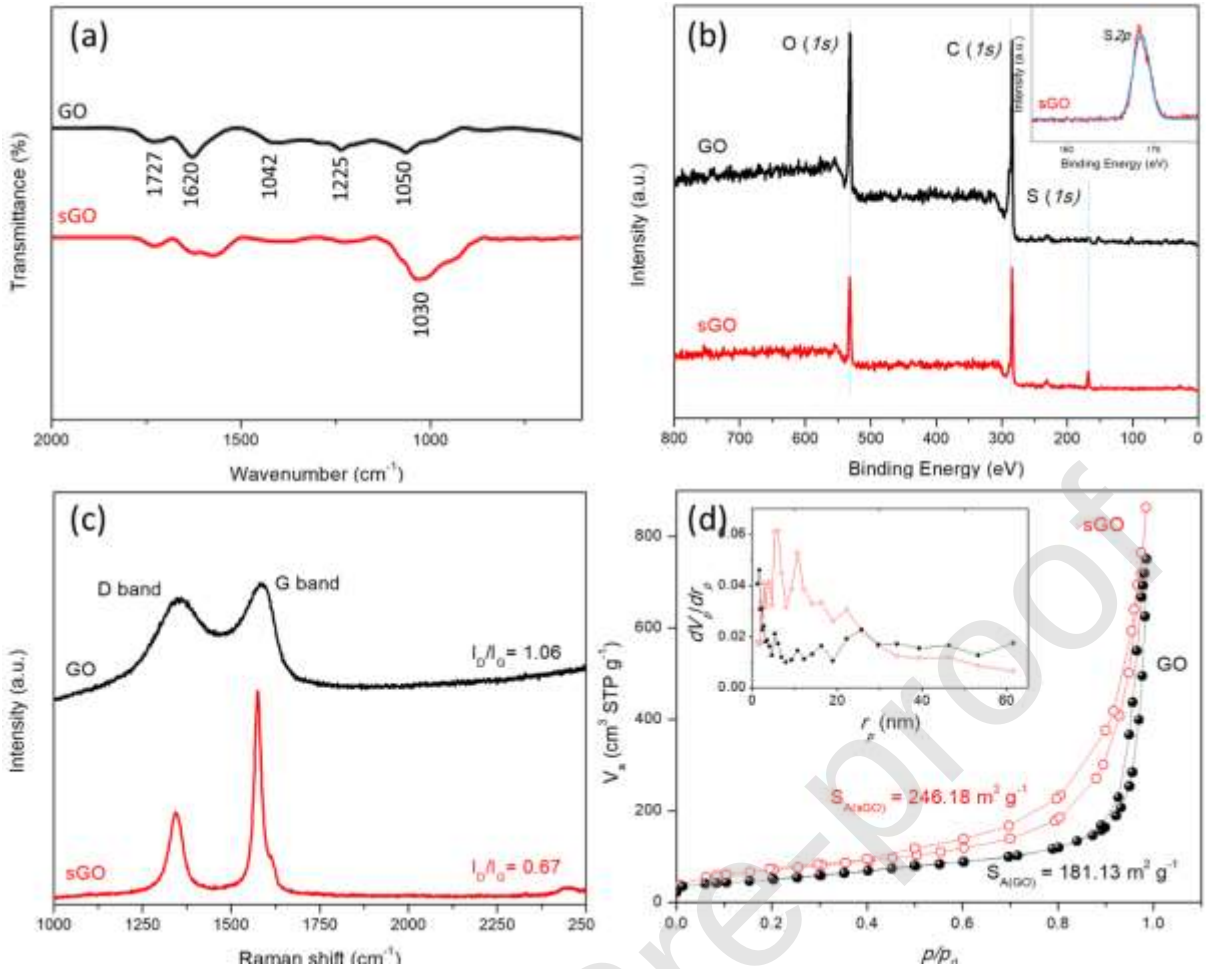

Figure 2 (a) FTIR, **(b)** XPS spectra, **(c)** Raman, and **(d)** N_2 adsorption-desorption isotherms of GO and sGO

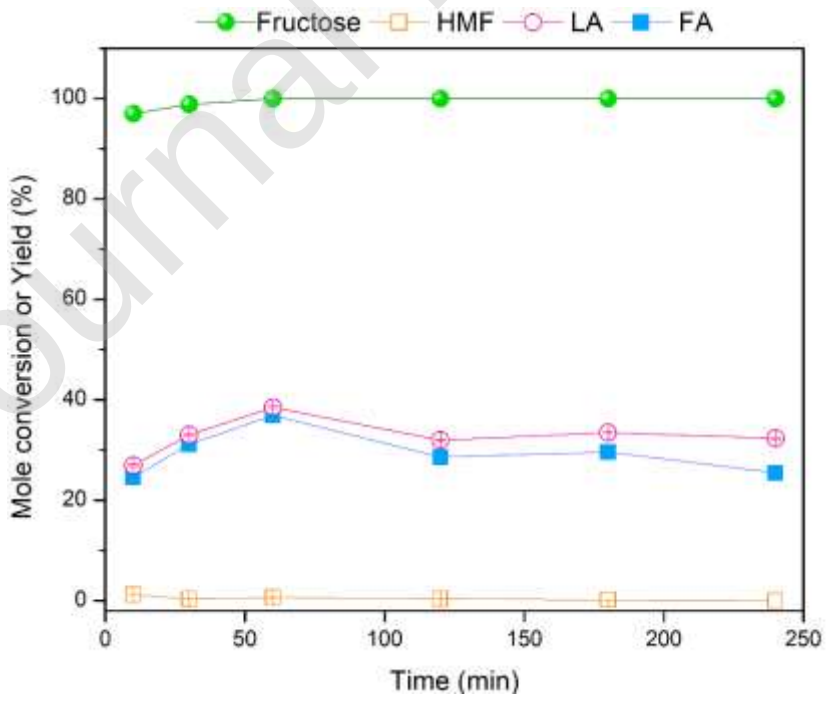

Figure 3 Effect of reaction time on fructose conversion and product yield (200 °C, 0.2 g catalyst, 4.5 g Fructose, 30 mL DI)

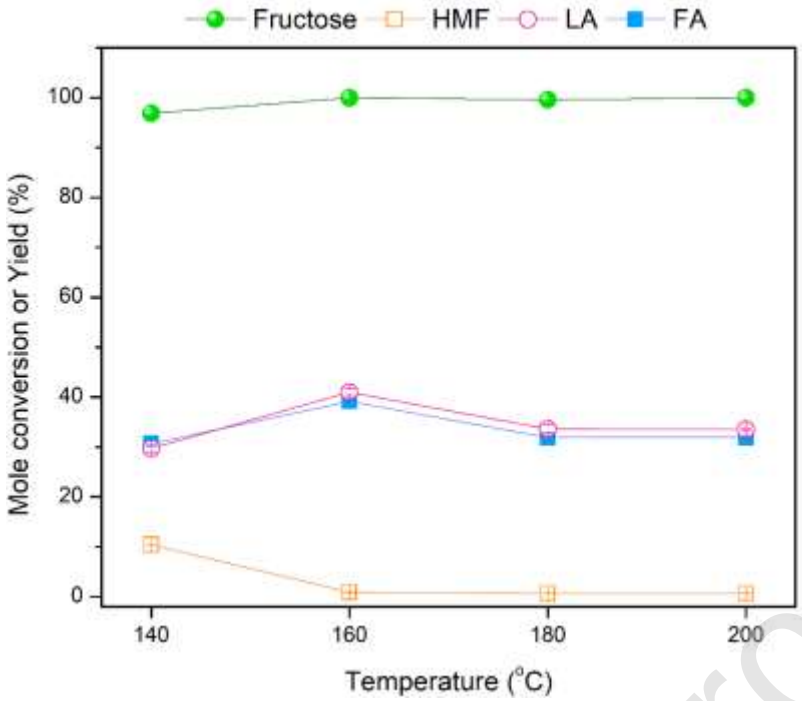

Figure 4 Effect of temperature on fructose conversion and product yield (1 h, 0.2 g catalyst, 4.5 g Fructose, 30 mL DI)

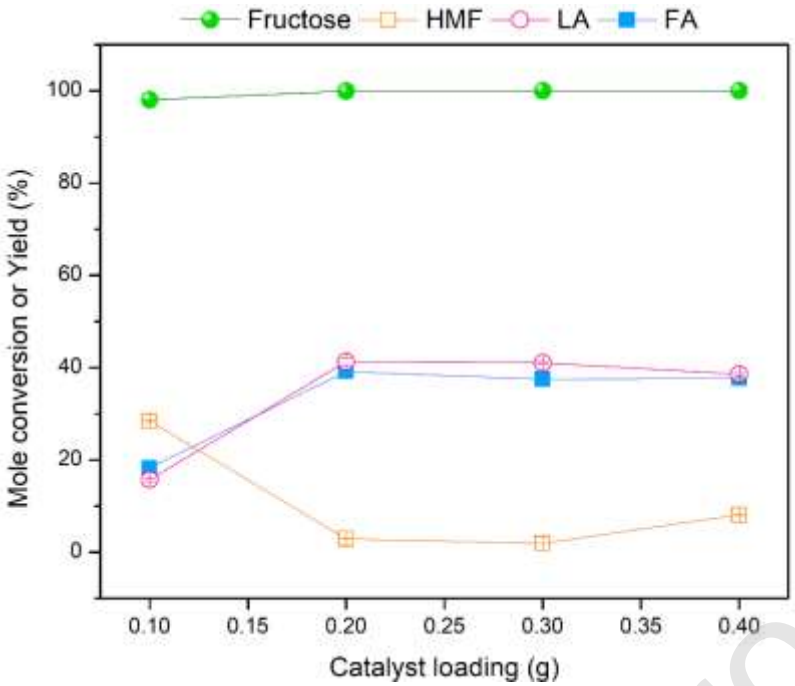

Figure 5 Effect of catalyst loading on fructose conversion and product yield (160 °C, 1 h, 4.5 g Fructose, 30 mL DI)

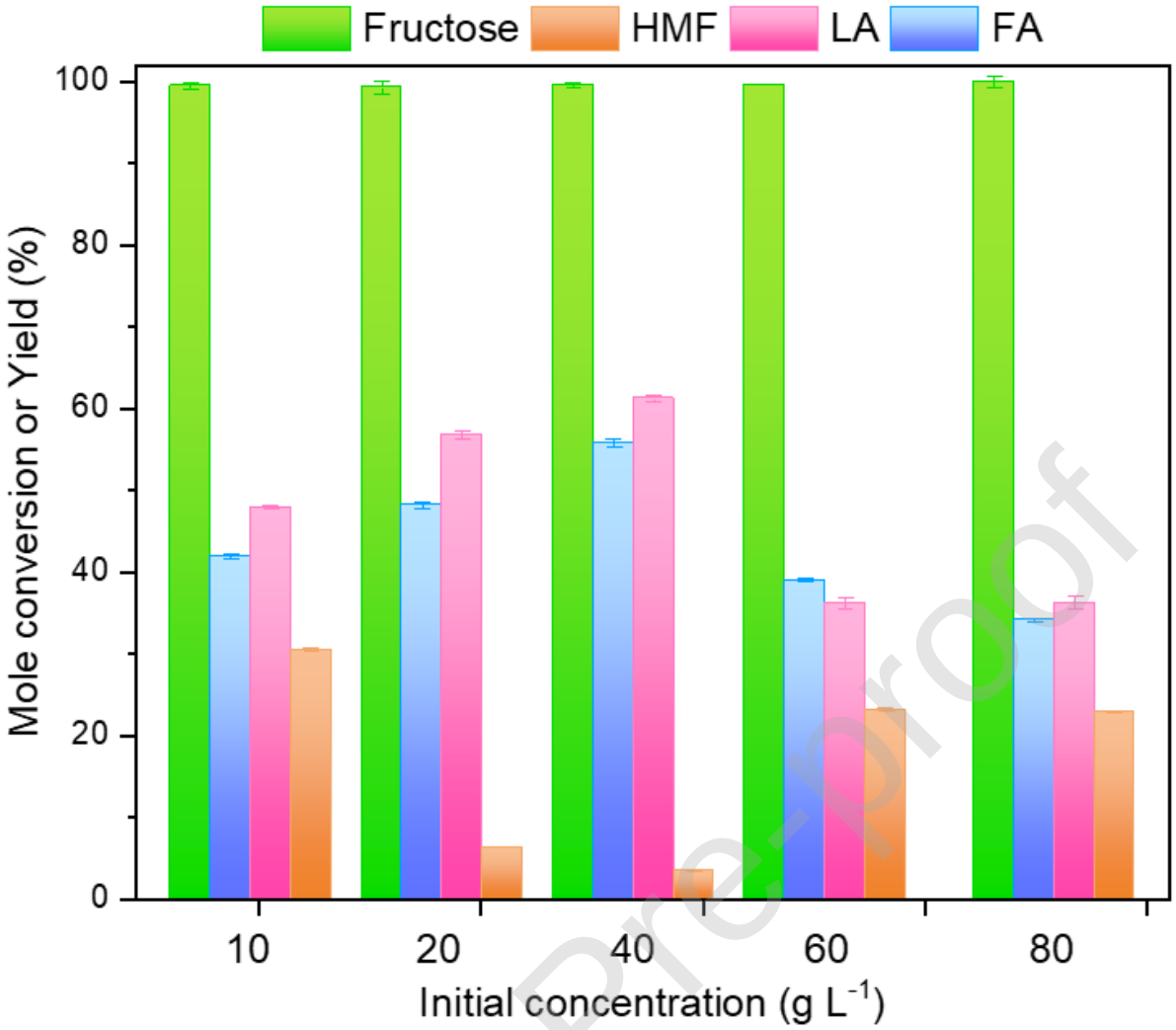

Figure 6 Effect of initial concentration of fructose on its conversion and product yield (160 °C, 1 h, F:C = 6 g g^{-1}, 30 mL DI)

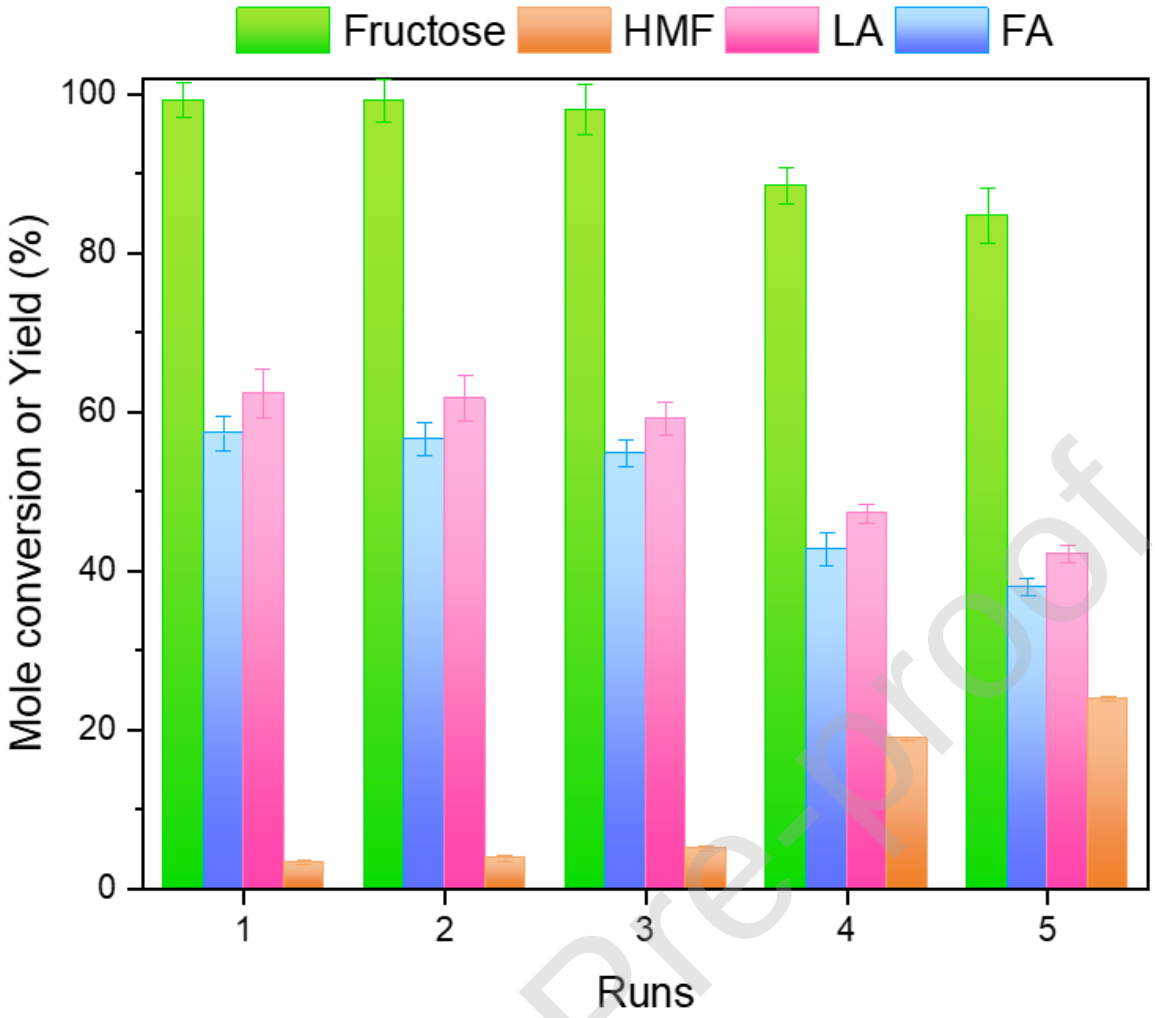

Figure 7 Effect of repeated runs using regenerated catalyst on its conversion and product yield (160 °C, 1 h, 0.2 g catalyst, 30 mL DI)

List of Tables

Table 1 Surface functional groups in GO and sGO

Table 2 Elemental analysis of GO and sGO

Table 3 Fructose (F) conversion to levulinic acid (LA) using various catalysts (C)

Table 4 Surface functional groups in sGO before (sGO-0), after one (sGO-1), and five runs (s GO-5) of fructose catalytic conversion.

Table 1 Surface functional groups in GO and sGO

Sample	**Sulfonic[a] (mmol g^{-1})**	**Carboxylic[b] (mmol g^{-1})**	**Phenolic[c] (mmol g^{-1})**	**Lactonic[d] (mmol g^{-1})**	**Total acid sites[e] (mmol g^{-1})**
GO	0.48	0.53	0.71	0.26	1.97
sGO	2.36	0.49	0.60	0.17	3.60

[a] From S content by elemental analysis. [b] Subtracted concentration of sulfonic groups from titration results with $NaHCO_3$. [c] Subtracted titration results using $NaHCO_3$ from calculated values of Na_2CO_3. [d] Subtracted titration results using Na_2CO_3 from the calculated values of NaOH. [e] From titration with NaOH

Table 2 Elemental analysis of GO and sGO

	% C	**% H**	**% O**	**% N**	**% S**
GO	42.11	2.94	53.00	0.15	1.54
sGO	41.79	4.11	46.34	0.18	7.58

Table 3 Fructose (F) conversion to levulinic acid (LA) using various catalysts (C)

Catalyst	**F : C (g g^{-1})**	**Solvent**	**Reaction conditions**	**LA yield (mol %)**	**References**
H_2SO_4	0.25	water	170 °C, 0.5 h (microwave reactor)	42.70 %	[2]
Amberlyst-15	0.75	water	120 °C, 36 h (batch reactor)	~52	[9]
LZY zeolite	1	-	140 °C, 15 h (batch reactor)	67.03	[32]
Dowex 50 × 8-100	1	50:50 mixture of	120 °C, 24 h	~72	[33]

resin		water/ γ-valerolactone	(batch reactor)		
Dowex 50 × 8-100 resin	1	water	120 °C, 24 h (batch reactor)	~58	[33]
H_2SO_4	1 8 . 8	γ-valerolactone	130 °C, 0.17 h (microwave reactor)	~70	[34]
H_2SO_4	0 . 1 8	water	140 °C, 1.67 h (batch reactor)	~74	[41]
sGO	6	water	160 ºC, 1h (batch reactor)	61.2	This study

Table 4 Surface functional groups in sGO before (sGO-0), after one (sGO-1), and five runs (sGO-5) of fructose catalytic conversion.

Sample	Sulfonic[a] (mmol g^{-1})	Carboxylic[b] (mmol g^{-1})	Phenolic[c] (mmol g^{-1})	Lactonic[d] (mmol g^{-1})	Total acid sites[e] (mmol g^{-1})
sGO-0	2.36	0.49	0.60	0.17	3.60
sGO-1	2.18	0.33	0.49	0.13	3.14
sGO-5	1.89	0.27	0.40	0.09	2.64

[a] From S content by elemental analysis. [b] Subtracted concentration of sulfonic groups from titration results with $NaHCO_3$. [c] Subtracted titration results using $NaHCO_3$ from calculated values of Na_2CO_3. [d] Subtracted titration results using Na_2CO_3 from the calculated values of NaOH. [e] From titration with NaOH